

Surface Boundary Conditions During Long-Term Climate Change Simulated by the UofTGSM 2.0 Framework

NWMO-TR-2023-10

August 2023

Gordan Stuhne and W. R. Peltier

University of Toronto, Department of Physics

nwmo

NUCLEAR WASTE
MANAGEMENT
ORGANIZATION

SOCIÉTÉ DE GESTION
DES DÉCHETS
NUCLÉAIRES



Nuclear Waste Management Organization

22 St. Clair Avenue East, 6th Floor

Toronto, Ontario

M4T 2S3

Canada

Tel: 416-934-9814

Web: www.nwmo.ca

Surface Boundary Conditions During Long-Term Climate Change Simulated by the UofTGSM 2.0 Framework

NWMO-TR-2023-10

August 2023

Gordan Stuhne and W. Richard Peltier
University of Toronto, Department of Physics

This report has been prepared under contract to NWMO. The report has been reviewed by NWMO, but the views and conclusions are those of the authors and do not necessarily represent those of the NWMO.

All copyright and intellectual property rights belong to NWMO.

Document History

Title:	Surface Boundary Conditions During Long-Term Climate Change Simulated by the UofTGSM 2.0 Framework		
Report Number:	NWMO-TR-2023-10		
Revision:	R00	Date:	August 2023
University of Toronto, Department of Physics			
Authored by:	Gordan Stuhne and W. Richard Peltier		
Verified by:	W. Richard Peltier		
Approved by:	W. Richard Peltier		
Nuclear Waste Management Organization			
Verified by:	Eric Sykes		
Reviewed by:	Eric Sykes, Paul Gierszewski and Alec Blyth		
Accepted by:	Andrew Parmenter		

ABSTRACT

Title: Surface Boundary Conditions During Long-Term Climate Change Simulated by the UofTGSM 2.0 Framework
Report No.: NWMO-TR-2023-10
Author(s): Gordan Stuhne and W. Richard Peltier
Company: University of Toronto, Department of Physics
Date: August 2023

Abstract

This report provides the technical background to the creation of the updated glacial surface boundary condition (BC) dataset that was recently provided to NWMO. The dataset was computed using version 2.0 of the University of Toronto Glacial Systems Model (UofTGSM), which improved upon UofTGSM 1.0 by incorporating an updated Parallel Ice Sheet Model (PISM) ice dynamical kernel that now includes dynamical coupling between ice sheets and surface lakes. The resulting dataset was found to be broadly consistent with the previously provided UofTGSM 1.0 dataset, although preliminary investigations suggest that coupling to lake dynamics may increase sensitivity to model parameters.

TABLE OF CONTENTS

	<u>Page</u>
ABSTRACT	iii
1. INTRODUCTION	1
2. METHODOLOGY	4
2.1 Ice Sheet Dynamics with Data Assimilation	4
2.2 GIA-Based and Lake Dynamical Surface Hydrology	5
2.3 New Reference Solution Parameters	8
3. DISCUSSION	11
4. SUMMARY AND CONCLUSIONS	14
REFERENCES	17
APPENDIX A: DATA FILE CONTENTS.....	20

LIST OF FIGURES

	<u>Page</u>
Figure 1: Representation of UofTGSM 1.0 water surfaces (A, ocean only) compared to more general UofTGSM 2.0 representations including lakes that are fully filled (B) and partly filled (C).	6
Figure 2: Comparisons of frames overlying ice thickness, ice shelf thickness, and lake depth at 12.5kyr BP, between UofTGSM 1.0 (top frames) and UofTGSM 2.0 (bottom frames), and between f0050rn001 (left frames) and f0050rn003 (right frames).....	12
Figure 3: LGM ice thickness deviations in the UofTGSM 2.0 f0050rn003 solution (upper right), the UofTGSM 1.0 f0050rn001 solution (lower left), and the UofTGSM 1.0 f0050rn003 solution (lower right), all with respect to the UofTGSM 2.0 f0050rn001 reference solution (upper left).	13
Figure 4: Comparisons of basal meltwater production rate at 12.5kyr between UofTGSM 1.0 (top frames) and UofTGSM 2.0 (bottom frames), and between f0050rn001 (left frames) and f0050rn003 (right frames).	15

LIST OF TABLES

Table 1:	New parameters arising from lake dynamics in PISM-LakeCC, with values used in reference dataset.	7
Table 2:	Ensemble parameters varied in the sensitivity analyses, with descriptions, units, ranges, and SP15 values.	10
Table 3:	Spatiotemporal fields provided in the netCDF data file, with corresponding unit attributes and combined long name and comment attributes.	21

1. INTRODUCTION

The potential for future continental-scale glaciation is an important consideration in the long-term evolution of sites selected for long-term storage of used nuclear fuel that will remain radioactive over timescales considerably longer than the typical glacial cycle (~ 100 kyr). It is reasonable to presume that typical patterns and extreme events in ice sheet evolution recur across glacial cycles, and studies of associated surface boundary conditions (BCs) have typically used the last, observationally well-evidenced glacial cycle as a model for future cycles. The University of Toronto GSM group has previously provided NWMO with a number of surface BC datasets derived through a combination of ice-sheet simulation, data assimilation, and glacial isostatic adjustment-based (GIA-based) reconstruction of ice thickness. The overall framework is referred to as the University of Toronto Glacial Systems Model (UofTGSM), and Peltier (2006, 2008, 2011) (hereafter P_{yy}) detailed the creation of initial datasets based upon an earlier version of the framework. Stuhne and Peltier (2015a, 2016a) (hereafter SP15 and SP16) then described an updated dataset and sensitivity analyses based upon the formally released UofTGSM 1.0 framework, which made major changes to the ice-dynamical models and modeling protocols used in the earlier, unreleased versions. The present work describes a preliminary version of a new dataset that derives from the latest version of the framework (UofTGSM 2.0), which retains the data formats and basic numerical modeling protocols that were established in SP15,16.

As introduced in UofTGSM 1.0, the basic modeling protocols make use of a widely-adopted and well studied community ice sheet model (the Parallel Ice Sheet Model, or PISM; Winkelmann et al., 2011; Bindschadler et al., 2013; Nowicki et al., 2013a,b), with model parameters and inputs that effectively combine the SeaRISE protocol with a data assimilation technique that nudges ice thickness towards the ICE-6G_C reconstruction of Argus et al. (2014) and Peltier et al. (2015) at time-scales of $\tau_f = 20, 100, 200,$ and 1000 years. The rationale for nudging is extensively discussed in SP15,16 and related journal publications (Stuhne and Peltier, 2015b, 2016b), and stems from the fact that hindcasts arising from naïve exploration of ice model parameter spaces generally fail to reproduce observational evidence of the last glacial cycle, and even to reasonably reconstruct terminal deglaciation leading up to modern conditions. Although parametric studies may theoretically quantify how intrinsic nonlinear dynamics causes unpredictable evolutionary variability between glacial cycles, it has to be recognized that model accuracy is primarily limited in practice by gross uncertainties in our knowledge of crucially relevant surface and climatological BCs. To focus attention upon results that reflect key elements of realism, early UofTGSM simulations enforced consistency with the observationally-based ice-margin chronologies of Dyke (2004) through application of margin forcing (see Tarasov and Peltier, 1997, 1999, 2000, 2002, 2003, 2004, 2007) (hereafter TP_{yy}). Margin forcing amounted to data assimilation, and was augmented by application of Bayesian techniques to the tuning of some other discrete model parameters. In spite of

these innovations, however, results were consistently poorer fits to observations than the results of pure GIA-based reconstructions of ice thickness history (Peltier, 1974, 1976a,b; Peltier and Andrews, 1976; Farrell and Clark, 1976; Clark et al., 1978; Peltier et al., 1978; Peltier, 1998, 2007; Peltier et al., 2015). Beyond replacing the custom developed and technically dated ice dynamics of the early UofTGSM with the PISM 0.6 model kernel, UofTGSM 1.0 incorporated explicit data assimilation that modified local mass balances in such a way as to nudge ice thickness towards observationally consistent histories. Nudging eliminated the rationale for Bayesian tuning of parameters, because simulations were designed from the outset to be dynamically “smoothed” versions of GIA-based reconstructions. In the absence of concerns about small parameter changes causing gross deviations from the observationally consistent ice thickness history, our setup allowed for systematic analysis of the sensitivity of surface BCs to model parameters (including the “smoothing” time constant, τ_f , which controls the degree to which ice thickness can dynamically deviate from the reference history).

The current UofTGSM 2.0 framework incorporated a host of technical improvements over UofTGSM 1.0 simply by upgrading the PISM 0.6 ice dynamical kernel to PISM 1.2.1. Beyond bringing the ice dynamical component of the framework up to the current state-of-the-art, the upgrade allows for study of the sensitivity of UofTGSM 1.0 simulations to an accumulation of model changes. Most of the changes reflected in PISM 1.2.1 implement incremental improvements upon model physics and parameterizations that were already well represented in PISM 0.6, but there is also a crucial addition of physics pertaining to the formation and evolution of proglacial lakes that have a very significant impact upon surface BCs. The efficient geometric lake filling algorithm was first described by Hinck et al. (2020) independently of ice dynamical coupling, and then incorporated into a PISM module implementing a coupled dynamical lake simulation technique (Hinck et al., 2022). The standalone geometric technique improves upon the rudimentary water column redistribution approach that SP15,16 applied to diagnosing lake depths through postprocessing of UofTGSM 1.0 simulations. Lake structure predicted by postprocessing of completed simulations cannot represent the influence that inferred proglacial lakes would have had upon the simulated ice dynamics, and the full complexities of dynamical lake-ice sheet coupling have only recently begun to be discussed in the literature on numerical methods. The much earlier studies of Tarasov and Peltier (2005, 2006) referred to the UofTGSM framework having a dynamically coupled representation of surface drainage interacting with ice sheets, and NWMO received lake depth information simulated by this feature in early time-series-based surface BC datasets. The caveat is that the above-cited science-focussed publications just provide a non-technical summary of methods that were acknowledged to have been heavily tuned for the simulation of Arctic freshwater forced Younger Dryas cold reversals, without technical documentation or validation that would have been needed to assess their more general applicability. As implemented in the publicly available software structure of PISM 1.2.1, the approach of Hinck et al. (2020, 2022) became the

basis for addressing these issues in UofTGSM 2.0.

Although it is clearly optimal in principle to simulate surface drainage with full dynamical coupling to ice sheet evolution, there are also practical benefits to a decoupled postprocessing approach in which simulated ice-sheet dynamics just provide one-way geometric and mass balance inputs for surface drainage simulations. Most significantly, postprocessing allows for surface drainage at selected discrete time levels to be computed at spatial resolutions that would be too fine to support computationally tractable coupled continental scale glacial simulations. Some capacity to estimate accurate surface drainage is particularly important, because lake levels may be affected by river drainage networks that often depend, in turn, upon very small-scale structures like narrow channels and dams. The methods of Hinck et al. (2022) make no attempt to accurately represent these very small scales, as would be required to accurately track how 2D river networks distribute meltwater and precipitation between lakes occurring within drainage basins that discharge surface water from large areas into the ocean. Simulation of lake surface evolution in relatively deep drainage basins does not hinge upon the same level of resolution, unless reconstructed lake surfaces are needed specifically to locally “flatten” high-resolution digital elevation models (DEMs) that serve as *inputs* to separate river routing and watershed structure prediction algorithms such as the multiple flow direction (MFD) technique of Holmgren (1994). Dynamical simulation of inter-lake and lake-ocean surface drainage fully coupled to lake surface and ice sheet dynamics is beyond the scope UofTGSM 2.0, and such simulation would in any case hinge upon surface characteristics beyond geometric topography (e.g., upon surface vegetation and other influences upon permeability, and upon subsurface flow patterns). MFD-type algorithms can accurately “predict” modern surface drainage patterns only when their modern high-resolution DEM inputs are hydrologically “conditioned” in such a way as to make results fit observed surface drainage patterns.

It is of interest that “conditioning” modern high-resolution DEMs in such a way as to enable MFD-type algorithms to “predict” modern river networks is rather akin to “conditioning” ice thickness history inputs to GIA-based methods with a view to matching evidence of past glaciation. The pure GIA-based methodology can, in this regard, be used as a procedure for “conditioning” modern high-resolution DEMs in such a way as to reconstruct the large scales of paleoclimate DEMs in which effective topography reflects ice-sheet surfaces over glaciated areas and related GIA of the bedrock surface elsewhere. Studies such as that of Wickert (2016) demonstrated the practicality and utility of applying MFD-type techniques to paleoclimate DEMs that result from such large-scale “conditioning” of modern high-resolution DEMs, but there is unfortunately no automatic way to generalize modern “conditioning” of *small-scale* DEM structure to paleoclimate states. Given that hydrological “conditioning” may introduce flat areas representing lake surfaces, there is at least one practical reason to use unconditioned high-resolution bedrock DEMs as a starting point for the reconstruction of paleoclimate DEMs. This acknowledges that heuristics addressing modern

small-scale complications are unlikely to apply to ice age conditions in which analogous complications likely came and went without leaving any signature in presently reconstructible conditioned DEM topography. This being said, one can, with appropriate awareness of the inherent problems, apply MFD-type techniques to ice-age conditions with modern small-scale bedrock topography. The UofTGSM 2.0 framework incorporated the relevant algorithms as postprocessing functions, through more general coupling to the widely used, open source GRASS GIS framework (Neteler et al., 2012).

Having described the improvements made to the UofTGSM 2.0 framework in general terms, this report will, in Section 2, go into more technical detail about the enhanced numerical methods and about the related expansion of the dynamical model parameter space considered in SP16. Section 3 will then present and discuss some selected results from the preliminary version 2.0 dataset, before a summary and conclusions are presented in Section 4.

2. METHODOLOGY

2.1 Ice Sheet Dynamics with Data Assimilation

Although the PISM-based thermomechanical ice-dynamical kernel of UofTGSM 2.0 has not been fundamentally modified from version 1.0, the software upgrade from PISM 0.6 to PISM 1.2.1 reflects some evolution in implementation details and in the associated suite of available options and parameters. It is important to note, in this regard, that our basic simulation protocols were designed from the outset for controlled studies of the effects of changing approximations of ice dynamics. Starting with the pure GIA-based ice history reconstruction, $I_{i6g}(\Omega, t)$, defined over 2D surface coordinates, Ω (e.g., latitude-longitude, or projections thereof) and time t , we deduce a derivative, dynamically “smoothed” solution, $I(\Omega, t)$, by solving a dynamical evolution equation of the following form: i.e.,

$$\begin{aligned} \frac{\partial I}{\partial t} + \nabla_{hor} \cdot \mathbf{Q} &= G_{surf} + \Delta G_{surf} \\ \Delta G_{surf} &= -\frac{I - I_{i6g}}{\tau_f}, \end{aligned} \tag{1}$$

in which τ_f defines the exponential time-scale over which I is nudged towards the GIA-based reconstruction through introduction of an anomalous surface mass balance, ΔG_{surf} , that modifies the base ice dynamical mass balance arising from horizontal divergence, ∇_{hor} , of horizontal ice flux, \mathbf{Q} , and from the scalar net effects, G_{surf} , of upper and lower surface mass balances. \mathbf{Q} and G_{surf} are obtained by solving the thermomechanical ice sheet equations in a generally 3D domain with lower boundary B (the bedrock surface topography at the base of the ice sheet) and upper boundary $B + I$. Externally supplied boundary conditions pertaining to basal geothermal

flux, surface climate, ice shelves, etc., are needed to fully determine the thermodynamic state of the ice sheet interior, as described by the prognostic evolution of a 3D scalar thermodynamic field, $\Theta(\Omega, z, t)$ (in which z is the vertical coordinate and Θ represents temperature or entropy). Ice velocity is diagnosed from l and Θ as needed to determine $\partial l/\partial t$ and $\partial \Theta/\partial t$ through more general diagnoses of \mathbf{Q} , 3D heat (or enthalpy) flux, and other dynamically relevant quantities. Quantities that are not directly relevant to the dynamical evolution of l and Θ can be obtained through postprocessing of completed solutions.

2.2 GIA-Based and Lake Dynamical Surface Hydrology

Figure 1 depicts how UofTGSM 2.0 refines the UofTGSM 1.0 representation of bodies of water, which level out at surfaces that deviate from the geoid, G (i.e., from absolute sea level), by constant increments, Δh . UofTGSM 1.0 supports only the circumstances depicted in Figure 1A, in which the ocean (with $\Delta h = 0$) is the only represented body of water. As discussed in SP15,16 and related journal publications for UofTGSM 1.0 (Stuhne and Peltier, 2015b, 2016b), the dynamical evolution of the bedrock surface, B , is determined by simplifying the sea level equation (SLE) based upon the assumption that “smoothing” deviations of l from the GIA-based reconstruction, l_{i6g} , do not affect the relative sea level (RSL, which is $G - B$ where $G > B$ and 0 elsewhere). The iterative SLE solution for ICE_6G (VM5a) can under these conditions be used to determine $\partial B/\partial t$ from $\partial l/\partial t$ without further time consuming and complex SLE iterations. The ice dynamical component of UofTGSM 2.0 represents the evolution of lakes with non-zero offset from the geoid, G , but this logic is not coupled to the SLE component in the manner that would theoretically be required if lakes had masses comparable to the major ice sheets. Insofar as the SLE solver is concerned, the simulation state continues to be defined by configuration shown in Figure 1A.

Figure 1B depicts the special circumstances in which potential lake basins are consistently filled to the point of overflow, and in which precipitation anywhere on the surface will consequently be balanced by outflow to the ocean (i.e., with lake overflow running downslope to cause other lakes to overflow, until the overflow reaches the ocean). The assumption of completely filled lake basins is not unreasonable during deglaciations such as the one that terminated the last ice age, and a geometry-based postprocessing technique can bypass ice dynamics entirely in deducing surface hydrology associated with GIA-based ice thickness reconstructions. A more general method should, of course, do better by allowing for partly filled basins along the lines depicted in Figure 1C. $\Delta h'_1$ and $\Delta h'_2$ will in general vary with time due to meltwater production, precipitation, and evaporation causing basin fill levels to rise and fall. In the simple one-dimensional geometry shown in the Figure, an outflow “river” will begin to flow when a lake is filled past its overflow point (i.e., $\Delta h'_i = \Delta h_i$). Realistic representation of lake formation within continental-scale surface runoff from deglaciations naturally requires solving the much more complex two-dimensional problem,

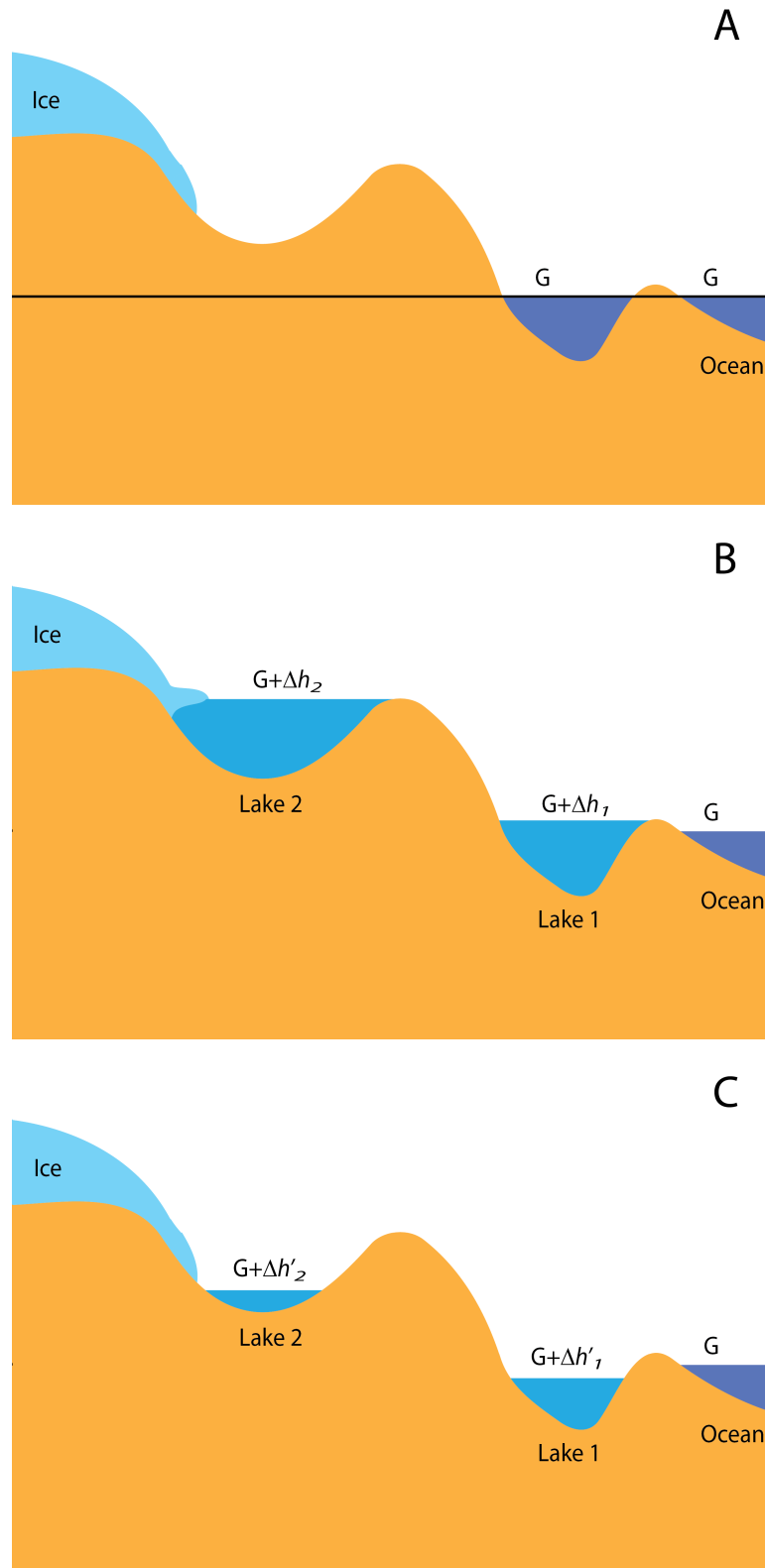


Figure 1: Representation of UofTGSMS 1.0 water surfaces (A, ocean only) compared to more general UofTGSMS 2.0 representations including lakes that are fully filled (B) and partly filled (C).

Parameter	Description (units)	Value
z_{\min}	Minimum lake level (m)	−300
z_{\max}	Maximum lake level (m)	1000
Δz	Lake level spacing (m)	4
F_{\max}	Maximum lake fill rate (m/year)	1
l_{\min}	Minimum thickness for ice cover (m)	10
l_{crit}^L	Critical ice thickness for lake ice calving (m)	50
N_{filt}	Lake filter size (cell count)	4
N_{iter}	Maximum number of LakeCC iterations	5
Δt_{upd}	Max time between LakeCC updates (years)	0

Table 1: New parameters arising from lake dynamics in PISM-LakeCC, with values used in reference dataset.

which apparently was not addressed in the literature until the recent development of the LakeCC algorithm by Hinck et al. (2020, 2022). The technical details are discussed at length in the cited publications and implemented in the open source PISM 1.2.1 software (which is specifically named PISM-LakeCC in the literature discussing the new lake component, but referred to hereafter as a PISM upgrade that also includes other enhancements over PISM 0.6), and we will just recall, as discussed in Section 1, that coupled lake dynamical simulation does *not* encompass coupling to dynamic MFD-type reconstruction of 2D river networks and watersheds.

The additional technical complexity arising from incorporation of the LakeCC algorithm into PISM naturally gave rise to additional tunable dynamical parameters that are summarized in Table 1. The Table lists the relatively intuitive descriptions of the parameters, which are labelled by the listed mathematical symbols, and take the listed values in the preliminary reference simulations that are discussed herein (see Hinck et al., 2020, 2022, for further discussion of parameters). With reference to Figure 1C, the evolution of lake surface displacements, $\Delta h'_i$, can, in the absence of full dynamical coupling to an MFD-based river and watershed model, be represented in terms of prescribed fill rates, F_i : i.e.,

$$\frac{\partial \Delta h'_i}{\partial t} = F_i,$$

for F_i limited by the maximum fill rate parameter, F_{\max} . The discrete algorithm requires associating the lake surface displacement with an integral value,

$$L_i \equiv \left\lfloor \frac{\Delta h'_i}{\Delta z} \right\rfloor,$$

in which L_i is defined as a positive or negative number of Δz -sized steps away from the geoid, and

constrained to lie within the limits

$$L_{\min} \leq L_i \leq \left\lfloor \frac{z_{\max}}{\Delta z} \right\rfloor,$$

for L_{\min} defined by

$$L_{\min} \equiv \left\lfloor \frac{\max(z_{\min}, B)}{\Delta z} \right\rfloor.$$

Each discrete horizontal grid cell of the ice dynamical model is deemed to be part of a lake if $L_i > L_{\min}$, but 2D lakes are filtered out (i.e., L_i is set to L_{\min} for all of their cells) if they are so small that there is not at least one lake cell with at least N_{filt} neighboring cells that are also in the lake. The algorithmic interaction between ice sheets and lakes requires that 2D simulation cells be treated as ice free for $l < l_{\min}$, and that floating ice shelves on lakes be rapidly calved for $l > l_{\text{crit}}^L$ (with this latter parameter playing the same role as l_{crit} in the ocean ice shelf parameterization). Lake level adjustments are limited to N_{iter} LakeCC iterations, and run no later than Δt_{upd} after the last adjustment (with the default, $\Delta t_{\text{upd}} = 0$, signifying that LakeCC runs more-or-less at every ice dynamical model time step).

2.3 New Reference Solution Parameters

Beyond the new lake dynamics-related parameters listed in Table 1, PISM 1.2.1 expanded the PISM 0.6 parameter space by introducing various new technical parameters pertaining to new options and parameterizations. For purposes of running new experiments, these were generally kept at default values that are documented in the open source software and options files, and that need not be explicitly discussed herein (the specific branch at which LakeCC is incorporated may be accessed at <https://github.com/sebhinck/pism-pub/releases>). We did, however, discover that a small number of physically insignificant PISM 0.6 numerical parameters began to have a practical impact upon simulation management when we attempted to reproduce ensembles of simulations prescribed by augmenting SP16 parameter values with lake dynamics described by Table 1 parameter values. A majority of simulations with added lake dynamics exhibited failure due to numerical instability, and various unsuccessful attempts to correct the issue led us to suspect a bug in the relatively newly implemented lake dynamics module of PISM. After personal communications with Sebastian Hinck, we learned, however, that these random numerical instabilities reflected a known shortcoming of the spatial discretization by which the base PISM model distinguished ice-covered and ice-free cells. We were, in this regard, unknowingly fortunate to have completed the extensive parameter studies and sensitivity analyses described in SP15,16 without encountering the issue. In hindsight, it appears that GIA-based nudging stabilized simulations by keeping ice sheet geometry relatively simple and free from certain unpredictable complex configurations involving thin ice. The addition of lake dynamics appears to compromise the stabilizing

effect of nudging, although it may be fortuitous even that a substantial fraction of our solutions remained stable over glacial cycles after being initialized by means of naive automatic parameter setting. The failure rate was in any case much too high to allow for the analyses of SP15,16 to be straightforwardly expanded upon through script-based automation of parameter-setting, model execution, and postprocessing for hundreds of analogous cases.

According to Hinck, the accepted PISM community “fix” for the aforementioned numerical instability issue requires re-starting failed simulations at earlier time levels, with non-physical numerical parameter adjustments aimed at producing a computationally different progression of time-steps - specifically, an alternative progression that will hopefully proceed to the intended simulation stop time. One way of numerically perturbing a simulation that has failed, while also damping any previously built up noise in the extended simulation, involves increasing the maximum diffusivity, D_{\max}^{SIA} , in the SIA model stress balance. It must be noted, however, that numerical noise is a symptom, rather than the root cause, of numerical instabilities that cannot be generically suppressed by generalized use of the maximum acceptable numerical diffusivity. Running an ensemble with high D_{\max}^{SIA} would block perturbation strategies based on further increases in this parameter when many simulations fail nevertheless. Even if a restarted and numerically perturbed simulation also fails, however, it will presumably gain some ground, and thereby give its successor an improved chance of progressing to completion. Such a manually intensive approach is tolerable if the focus is upon completing and analyzing a handful of solutions, but there is a practical threshold at which it becomes infeasible to manually manage large simulation ensembles with dozens, or hundreds, of numerically unstable cases. Barring some resolution of the underlying shortcoming in the PISM discretization, a practical approach would appear to require automation of the procedures for numerically re-parameterizing and restarting failed simulations. Setting this notion aside as an eventual goal, we began, as in SP15, by focussing attention upon a handful of potential reference solutions. Parameter values for two candidates are listed in Table 2, which adds columns to the listing and description of ensemble-varying parameters in Table 1 of SP16. The simulations of interest are f0050r001 and f0050r003 from the f0050rxxx of SP16 (row 6 in the ensemble listing in Table 2). f0050r001 was ultimately selected as the basis for the preliminary reference dataset, but f0050r003 is also considered herein because results from it were presented in some NWMO forums, and because it is of interest to document the process leading up to the relatively arbitrary choice of f0050r001 (which occurred because f0050r003 happened to exhibit the aforementioned random instability issue when the adaptive time-stepping scheme was told to save restart data at the time-levels required for diagnoses of permafrost thickness).

With regards to the reference solution selection reflected in Table 2, the decision to increase the reference nudging time constant from $\tau_f = 100$ years (as in SP15) to $\tau_f = 200$ years reflects the discovery that Laurentide and Fennoscandian ice-sheet simulations reasonably maintain the observational fit quality of the ICE_6G_C (VM5a) reconstruction with less mass balance adjust-

Parameter	Description (units)	SP16 range	SP15 value	f0050rn001 value	f0050rn003 value
τ_f	Nudging time constant (years)	20 - 1000	100	200	200
A_{SIA}	SIA ice hardness factor	1.5 - 7.0	5.6	3.97	6.673
A_{SSA}	SIA ice hardness factor	0.5 - 6.0	1.0	5.153	4.279
l_{crit}	Critical ice thickness for calving (m)	150 - 350	250	345.544	280.076
U_{ref}	Velocity parameter in sliding law (m/s)	25.0 - 300.0	100	180.372	53.014
ϕ_{min}	Till geometry minimum angle (degrees)	5.0 - 25.0	5	17.503	12.091
ϕ_{max}	Till geometry maximum angle (degrees)	27.0 - 42.0	40	40.812	35.405
B_{min}	Till geometry elevation minimum (m)	-400 - -10	-300	-74.736	-64.119
B_{max}	Till geometry elevation maximum (m)	0 - 800	700	497.574	59.890

Table 2: Ensemble parameters varied in the sensitivity analyses, with descriptions, units, ranges, and SP15 values.

ment (or, more “smoothing”) than Greenland and Antarctic ice-sheet simulations (which were the initial reference cases in SP15). Insofar as the other parameters are concerned, the $f_{0050r_{n001}}$ and $f_{0050r_{n003}}$ values were randomly generated within the SP16 ensemble parameter range. These simulations were retrospectively selected for closer consideration because the associated numerical analyses were easily manageable and found to produce qualitatively typical results. As noted above, further technical work will be needed to enable comprehensive comparisons with SP15,16.

3. DISCUSSION

An assortment of UofTGSM 1.0 simulations from the ensembles in SP16 was successfully reproduced in UofTGSM 2.0, with coupling to lake dynamics described by the parameters in Table 1. Notwithstanding the aforementioned challenges impeding the complete automatic reproduction of all previous results, initial examinations of the results that could be fully reproduced without extensive manual intervention broadly showed that the character of the UofTGSM 1.0-based dataset was not fundamentally altered by the introduction of new physics. The discussion in the present Section will selectively compare versions 1.0 and 2.0 of $f_{0050r_{n001}}$ and $f_{0050r_{n003}}$ simulations (of which the former is the basis for the new preliminary dataset), with a focus upon the 12.5 kyr BP time level at which there were favorable conditions for the formation of large proglacial lakes, and at which the ongoing widening of the Ice-Free Corridor between the Laurentide and Cordilleran Ice Sheets was precipitating a major reorganization of North American watersheds and river drainage networks. The surrounding period in the history of global deglaciation is the subject of a variety of scientifically interesting discussions that will be taken up in future, but the objective in the present document is simply to assess the consistency of surface BC datasets.

Figure 2 depicts the essential structures of non-vanishing grounded ice thickness, floating ice thickness, and lake depth, all overlaid on frames that also show the PISM model domain and the high resolution bedrock DEM. Representing the respective outputs of the UofTGSM 2.0 and 1.0 frameworks, the lower frames are clearly distinguishable from the upper frames on account of exhibiting prominent proglacial lakes with surfaces partly obscured by floating ice shelves. The realism of the simulated ice shelves is questionable, but the positions of the simulated proglacial lakes is geographically consistent with proxy evidence of the evolution of named prehistoric proglacial lakes (Agassiz, Chicago, Whittlesey, etc.). The presence of these additional features in the UofTGSM 2.0 simulations does not have a major impact upon the UofTGSM 1.0 grounded ice sheet, although Figure 2 does show some minor evidence of accelerated margin retreat. Within a particular UofTGSM framework version, the differences between $f_{0050r_{n001}}$ and $f_{0050r_{n003}}$ simulations (left and right frames, respectively) are more even more modest. The UofTGSM 1.0 versions of these simulations predict virtually identical ice sheets, although the UofTGSM 2.0 versions exhibit

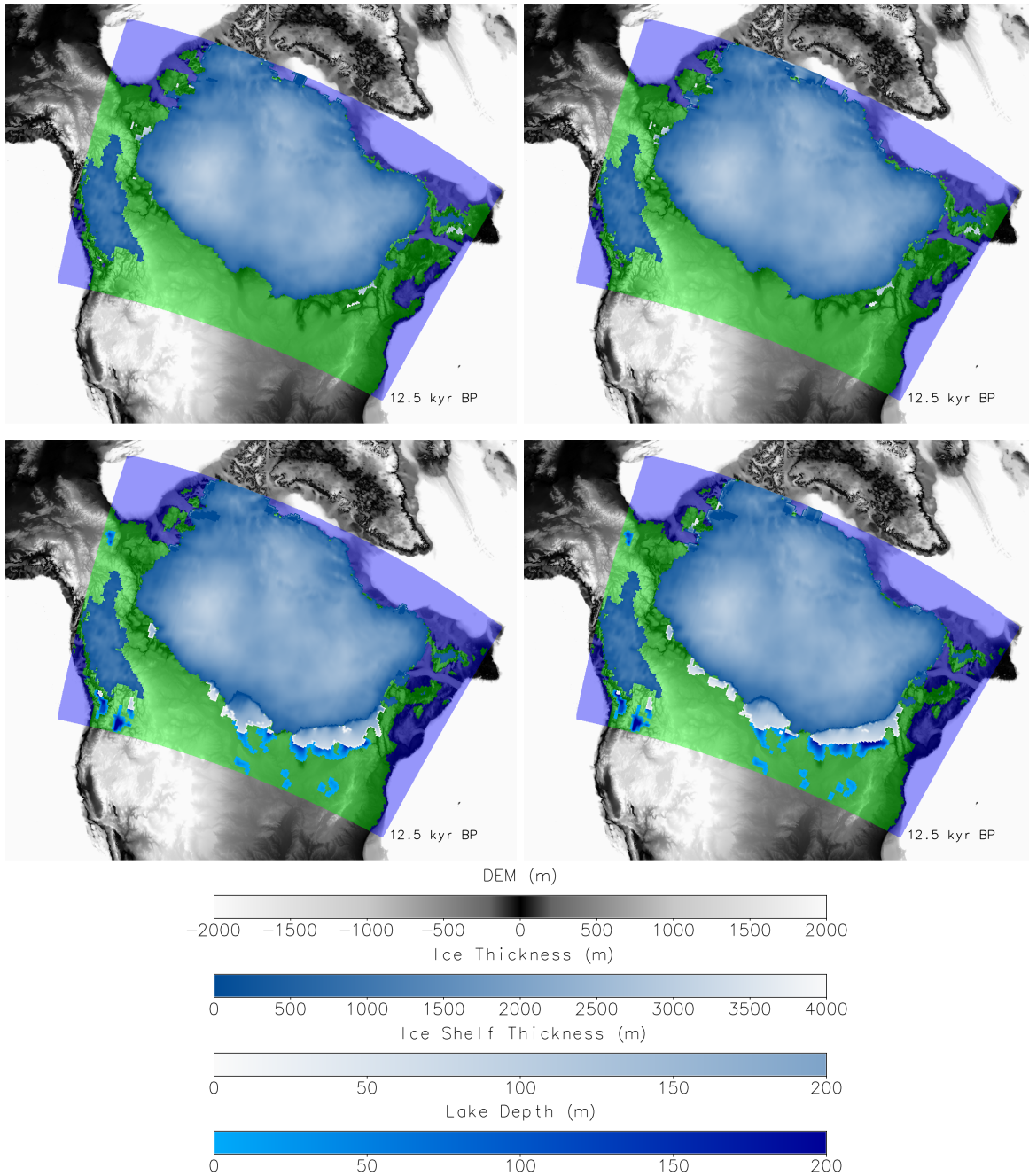


Figure 2: Comparisons of frames overlying ice thickness, ice shelf thickness, and lake depth at 12.5kyr BP, between UofTGSM 1.0 (top frames) and UofTGSM 2.0 (bottom frames), and between f0050rn001 (left frames) and f0050rn003 (right frames).

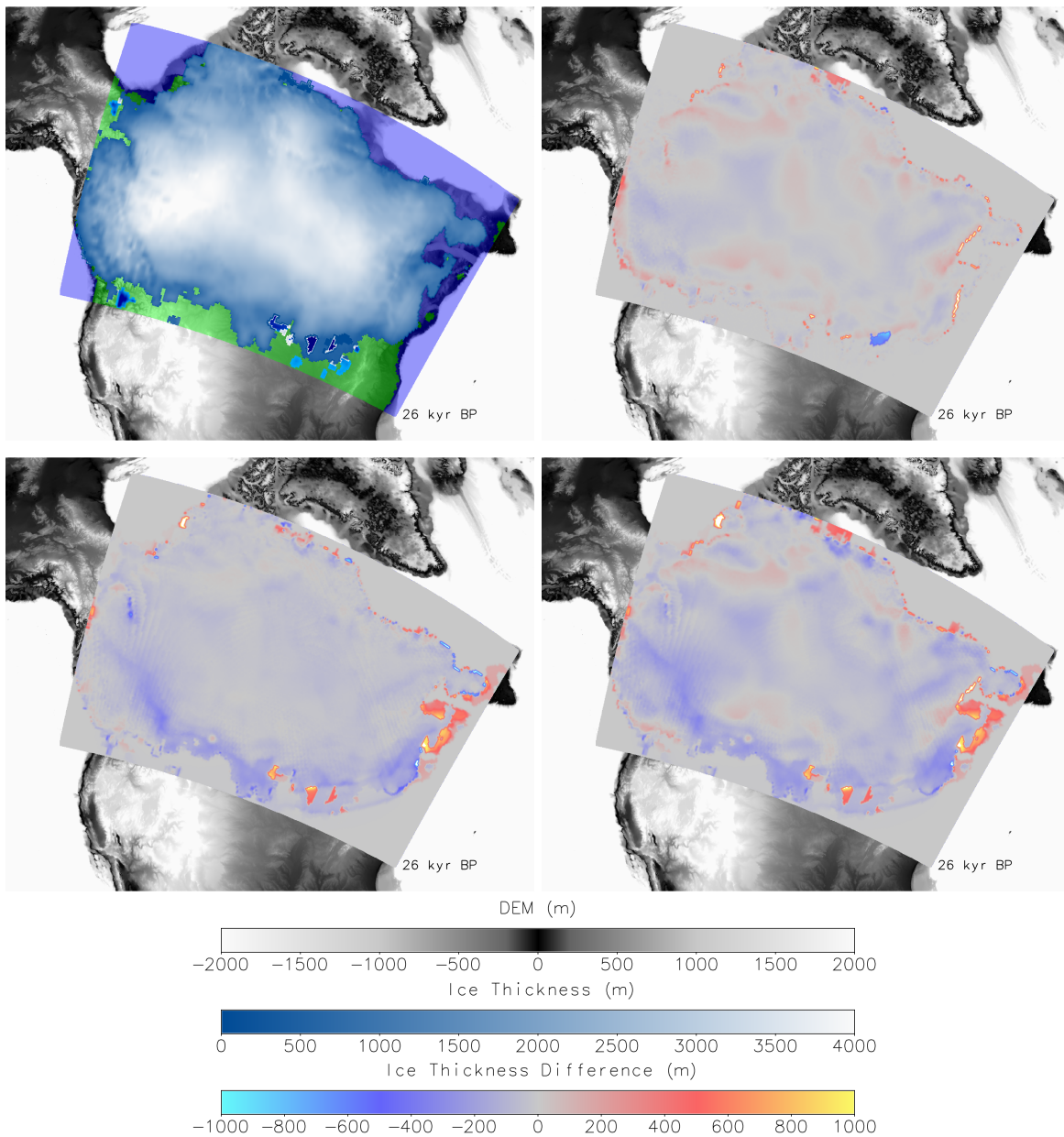


Figure 3: LGM ice thickness deviations in the UofTGS 2.0 f0050rn003 solution (upper right), the UofTGS 1.0 f0050rn001 solution (lower left), and the UofTGS 1.0 f0050rn003 solution (lower right), all with respect to the UofTGS 2.0 f0050rn001 reference solution (upper left).

clear differences in proglacial lake activity along the ice sheet margins.

To consider the crucial LGM time frame (when glaciation peaked at around 26 kyr BP) while also presenting a more quantitative view of the effects of shifting between model versions and ensemble instances, Figure 3 shows the f0050r001 UofTGSM 2.0 solution in the upper left corner (in the format of Figure 2) alongside the ice thickness deviations that result from shifting to the f0050r003 solution (right frames) and/or to the UofTGSM 1.0 model version (bottom frames). Deviations resulting from shifts along the two axes are minor and characterized by distinct patterns. Changing model versions has effects primarily at ice margins where there are occurrences of proglacial lakes and ice shelves, while changing ensemble parameters also affects the ice sheet interior thickness in a way that is reproducible between model versions. These results confirm that the new surface BC dataset is non-trivially sensitive to the overall modeling environment, but that this sensitivity does not significantly affect GIA-reconstructed extreme ice thicknesses in the interior of the ice sheet.

The previous technical reports (SP15 and SP16) included many figures and much associated discussion examining all of the various surface BC fields that were provided in the UofTGSM 1.0 dataset. More extensive material along these lines will likely prove to be useful when we are in a position to systematically reproduce the sensitivity analyses of SP16, but we will, in the present discussion, restrict ourselves to reexamination of just one diagnosed surface BC field: i.e., the distribution of basal meltwater production. Figure 4 depicts the relevant comparisons with the same frame arrangement as in Figure 1. Once again, the distinctions between f0050r001 and f0050r003 UofTGSM 1.0 simulations are clearly minimal. As is evident from the lower frames, coupling to lake dynamics in UofTGSM 2.0 amplifies discrepancies between the two ensemble members while causing both simulations to consistently exhibit enhanced meltwater production near the mouth of the St Lawrence river. As is especially evident in the f0050r003 solution, enhanced basal melting correlates with small-scale proglacial lake activity in Figure 2. These regional sensitivities were already predicted in Figure 20 of SP16, and appear now to have been intensified by the introduction of the additional physics. The details of this will become evident when we eventually embark upon systematic reproduction of the analyses of SP16, but our next priority is to develop scientific understanding by applying the UofTGSM 2.0 framework to open literature issues.

4. SUMMARY AND CONCLUSIONS

In summary, the UofTGSM 2.0 framework improved upon UofTGSM 1.0 by incorporating version 1.2.1 of the PISM ice dynamical kernel along with the LakeCC model for coupled dynamical simulation of proglacial lake evolution. Additional postprocessing tools allowing for MFD-type high-resolution analyses of rivers and watersheds have also been incorporated into UofTGSM 2.0. We

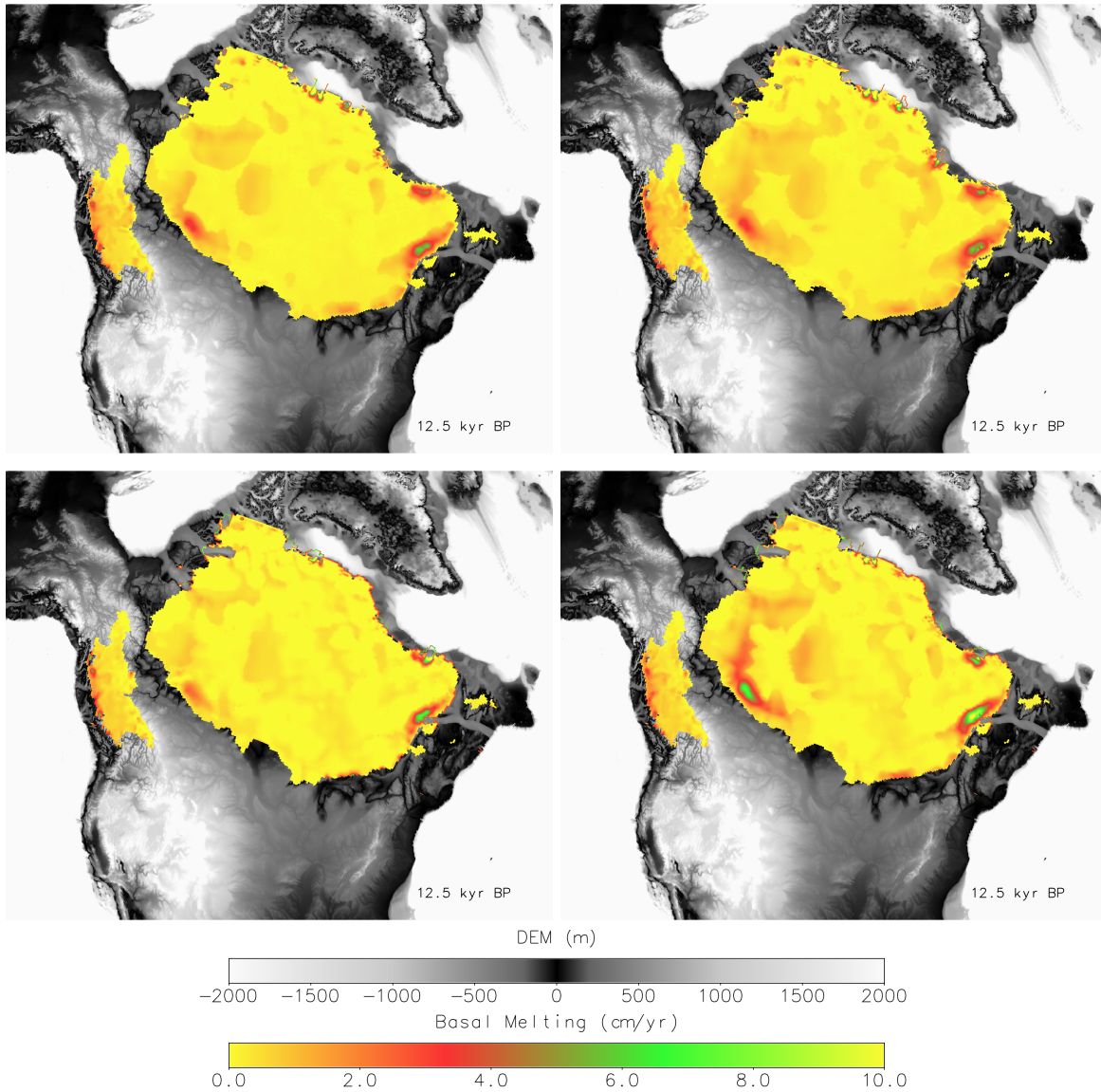


Figure 4: Comparisons of basal meltwater production rate at 12.5kyr between UofT-GSM 1.0 (top frames) and UofTGSM 2.0 (bottom frames), and between f0050rn001 (left frames) and f0050rn003 (right frames).

attempted to apply the updated framework to the automated reproduction of SP16 results within an expanded physical parameter space, but it was discovered that we had, in our earlier work, unknowingly and fortuitously avoided a known shortcoming that sometimes triggers random numerical instabilities tied to the PISM spatial discretization. Even though there are known workarounds for the issue, cumbersome manual corrections of large-simulation ensembles was put off in favor of more detailed consideration of reference solutions selected from the ensemble parameter space of SP15. UofTGSM 2.0 simulations are broadly consistent with their UofTGSM 1.0 analogues, except that introduction of coupled lake dynamics appears to increase sensitivity to model parameters (at least insofar as the selected new reference solution and one alternative solution are concerned).

The work discussed herein has verified that the UofTGSM 2.0 framework maintains general consistency with our earlier work while allowing for investigation of new physics. Outstanding tasks now include applying the new framework to publishable scientific analyses, and finding a way to automate the simulation restarts and adjustments that would otherwise have to be manually applied to sensitivity analyses involving hundreds of simulations. The results of these ongoing efforts will be reported in future publications and technical reports. In order to formally lay the groundwork for eventual comparisons with updated datasets, the interim dataset reported upon herein will be ascribed the identifier UTGSM2-2023 (based on the UofTGSM version and the year in which the dataset was produced).

REFERENCES

- Argus, D. F., W. R. Peltier, R. Drummond, and S. Moore (2014), The antarctic component of glacial isostatic adjustment model ICE-6G_C (VM5a) based upon GPS measurements of vertical motion of the crust, exposure age dating of ice thickness variations and relative sea level histories, *Geophys J. Int.*, 198, 537–563.
- Bindschadler, R. A., S. Nowicki, A. Abe-Ouchi, A. Aschwanden, H. Choi, J. Fastook, G. Granzow, R. Greve, G. Gutowski, U. Herzfeld, et al. (2013), Ice-sheet model sensitivities to environmental forcing and their use in projecting future sea level (the SeaRISE project), *Journal of Glaciology*, 59(214), 195–224.
- Clark, J. A., W. E. Farrell, and W. R. Peltier (1978), Global changes in postglacial sea level: a numerical calculation, *Quaternary Research*, 9(3), 265–287.
- Dyke, A. S. (2004), An outline of North American deglaciation with emphasis on central and northern Canada, *Developments in Quaternary Sciences*, 2, 373–424.
- Farrell, W., and J. A. Clark (1976), On postglacial sea level, *Geophysical Journal International*, 46(3), 647–667.
- Hinck, S., E. J. Gowan, and G. Lohmann (2020), Lakecc: a tool for efficiently identifying lake basins with application to palaeogeographic reconstructions of north america, *Journal of Quaternary Science*, 35(3), 422–432.
- Hinck, S., E. J. Gowan, X. Zhang, and G. Lohmann (2022), Pism-lakecc: Implementing an adaptive proglacial lake boundary in an ice sheet model, *The Cryosphere*, 16(3), 941–965.
- Holmgren, P. (1994), Multiple flow direction algorithms for runoff modelling in grid based elevation models: an empirical evaluation, *Hydrological processes*, 8(4), 327–334.
- Neteler, M., M. H. Bowman, M. Landa, and M. Metz (2012), Grass gis: A multi-purpose open source gis, *Environmental Modelling & Software*, 31, 124–130.
- Nowicki, S., R. A. Bindschadler, A. Abe-Ouchi, A. Aschwanden, E. Bueler, H. Choi, J. Fastook, G. Granzow, R. Greve, G. Gutowski, et al. (2013a), Insights into spatial sensitivities of ice mass response to environmental change from the SeaRISE ice sheet modeling project I: Antarctica, *Journal of Geophysical Research: Earth Surface*, 118(2), 1002–1024.
- Nowicki, S., R. A. Bindschadler, A. Abe-Ouchi, A. Aschwanden, E. Bueler, H. Choi, J. Fastook, G. Granzow, R. Greve, G. Gutowski, et al. (2013b), Insights into spatial sensitivities of ice mass response to environmental change from the SeaRISE ice sheet modeling project II: Greenland, *Journal of Geophysical Research: Earth Surface*, 118(2), 1025–1044.

- Peltier, W. (1974), The impulse response of a Maxwell Earth, *Reviews of Geophysics*, 12(4), 649–669.
- Peltier, W. (1976a), Glacial-Isostatic Adjustment—II. The Inverse Problem, *Geophysical Journal of the Royal astronomical society*, 46(3), 669–705.
- Peltier, W. (1976b), Glacio-isostatic adjustment-III. The inverse problem, *Geophysics Journal*, 46, 669–706.
- Peltier, W. (1998), Postglacial variations in the level of the sea: Implications for climate dynamics and solid-earth geophysics, *Reviews of Geophysics*, 36(4), 603–689.
- Peltier, W. (2007), *History of Earth rotation*, vol. 9, pp. 243–293, Elsevier Oxford.
- Peltier, W., and J. Andrews (1976), Glacial-Isostatic Adjustment—I. The Forward Problem, *Geophysical Journal of the Royal Astronomical Society*, 46(3), 605–646.
- Peltier, W., W. Farrell, and J. Clark (1978), Glacial isostasy and relative sea level: a global finite element model, *Tectonophysics*, 50(2), 81–110.
- Peltier, W. R. (2006), Boundary conditions data sets for spent fuel repository performance assessment, Tech. Rep. 06819-REP-01200-10154-R00, Department of Physics, University of Toronto, East Lansing, Michigan.
- Peltier, W. R. (2008), Phase I Long Term Climate Change Study, Tech. Rep. OPG 00216-REP-01300-00004-R00, Ontario Power Generation, <http://www.opg.com/generating-power/nuclear/nuclear-waste-management/Deep-Geologic-Repository/Documents/HPD/4.3.33.PhaseILongTermClimateChangeStudy.pdf>.
- Peltier, W. R. (2011), Long-term climate change, Tech. Rep. NWMO DGR-TR-2011-14, Department of Physics, University of Toronto, Toronto, Ontario.
- Peltier, W. R., D. F. Argus, and R. Drummond (2015), Space geodesy constrains ice age terminal deglaciation: The global ICE-6G_C (VM5a) model, *Journal of Geophysical Research: Solid Earth*, 119, 1–38.
- Stuhne, G. R., and W. R. Peltier (2015a), Surface boundary conditions during long-term climate change, Tech. Rep. NWMO-TR-2015-16, Department of Physics, University of Toronto, Toronto, Ontario.
- Stuhne, G. R., and W. R. Peltier (2015b), Reconciling the ICE-6G_C reconstruction of glacial chronology with ice sheet dynamics: the cases of Greenland and Antarctica, *Journal of Geophysical Research: Land Surface*, 120, 1841–1865.

- Stuhne, G. R., and W. R. Peltier (2016a), Sensitivity analyses of surface boundary conditions during long- term climate change, Tech. Rep. NWMO-TR-2016-19, Department of Physics, University of Toronto, Toronto, Ontario.
- Stuhne, G. R., and W. R. Peltier (2016b), Assimilating the ICE-6G.C reconstruction of the latest Quaternary ice-age cycle into numerical simulations of the Laurentide and Fennoscandian ice-sheets, *Journal of Geophysical Research: Land Surface*, submitted.
- Tarasov, L., and W. Peltier (1997), Terminating the 100 kyr ice age cycle, *Journal of Geophysical Research*, 102(D18), 21,665–21.
- Tarasov, L., and W. Peltier (1999), Impact of thermomechanical ice sheet coupling on a model of the 100 kyr ice age cycle, *Journal of Geophysical Research. D. Atmospheres*, 104, 9517–9545.
- Tarasov, L., and W. Peltier (2000), Laurentide ice sheet aspect ratio in models based on Glen's flow law, *Annals of Glaciology*, 30(1), 177–186.
- Tarasov, L., and W. Peltier (2002), Greenland glacial history and local geodynamic consequences, *Geophys. J. Int.*, 150, 198–229.
- Tarasov, L., and W. Peltier (2003), Greenland glacial history, borehole constraints, and Eemian extent, *J. Geophys. Res.*, 108(2143), 10–1029.
- Tarasov, L., and W. Peltier (2004), A geophysically constrained large ensemble analysis of the deglacial history of the North American ice-sheet complex, *Quaternary Science Reviews*, 23(3), 359–388.
- Tarasov, L., and W. Peltier (2005), Arctic freshwater forcing of the Younger Dryas cold reversal, *Nature*, 435(7042), 662–665.
- Tarasov, L., and W. Peltier (2006), A calibrated deglacial drainage chronology for the North American continent: evidence of an Arctic trigger for the Younger Dryas, *Quaternary Science Reviews*, 25(7), 659–688.
- Tarasov, L., and W. Peltier (2007), Coevolution of continental ice cover and permafrost extent over the last glacial-interglacial cycle in North America, *Journal of geophysical research*, 112(F2).
- Wickert, A. D. (2016), Reconstruction of north american drainage basins and river discharge since the last glacial maximum, *Earth Surface Dynamics*, 4(4), 831–869.
- Winkelmann, R., M. Martin, M. Haseloff, T. Albrecht, E. Bueler, C. Khroulev, and A. Levermann (2011), The Potsdam parallel ice sheet model (PISM-PIK)—Part 1: Model description, *The Cryosphere*, 5(3), 715–726.

APPENDIX A: DATA FILE CONTENTS

The reference dataset is provided in the netCDF format that is widely used for distributing and archiving two- and three-dimensional field data in atmospheric, oceanic, and other geophysical sciences. This Appendix provides a brief overview of the contents and internal documentation of the netCDF file, in which the dimensions $x = 200$, $y = 150$, and $time = 146$ prescribe the number of data points in the identically named one-dimensional arrays that prescribe nodes along the horizontal spatial, vertical spatial, and temporal axes (respectively). X and Y coordinates in meters are defined with respect to a polar stereographic projection over the standard WGS84 ellipsoid, with projection origin at 90 degrees north, standard parallel at 60 degrees north, and reference longitude at 120 degrees west. Time coordinates in years are defined with respect to the present. Table 3 summarizes the spatiotemporal prognostic and diagnostic field data that is provided in the dataset, with each row showing variable name, units attribute, and combined long name and comment attributes for a particular field. Further insights into the data can be obtained through application of standard public domain netCDF tools to the dataset file.

Field	Units	Long Name + Comment
bmelt	m year-1	ice basal melt rate from energy conservation and subshelf melt, in ice thickness per time positive basal melt rate corresponds to ice loss
climatic_mass_balance	kg m-2 year-1	surface mass balance (accumulation/ablation) rate
lake_depth	meters	lake depth
mask	meters	ice-type (ice-free/grounded/floating/ocean) integer mask
ocean_depths	meters	ocean depth
pthk	meters	z-level of T=0C isotherm in lithosphere temperature
taub_x	Pa	X-component of the shear stress at the base of ice this field is purely diagnostic (not used by the model)
taub_y	Pa	Y-component of the shear stress at the base of ice this field is purely diagnostic (not used by the model)
taud_x	Pa	X-component of the driving shear stress at the base of ice this is the driving stress used by the SSA solver
taud_y	Pa	Y-component of the driving shear stress at the base of ice this is the driving stress used by the SSA solver
tempbase	K	ice temperature at the base of ice
temppabase	Celsius	pressure-adjusted ice temperature at the base of ice
thk	m	land ice thickness
topg	m	bedrock surface elevation
ubar	m year-1	vertical mean of horizontal ice velocity in the X direction
uflux	m2 year-1	Vertically integrated horizontal flux of ice in the X direction
usurf	m	ice top surface elevation
uvelbase	m year-1	x-component of the horizontal velocity of ice at the base of ice
vbar	m year-1	vertical mean of horizontal ice velocity in the Y direction
vflux	m2 year-1	Vertically integrated horizontal flux of ice in the Y direction

Table 3: Spatiotemporal fields provided in the netCDF data file, with corresponding unit attributes and combined long name and comment attributes.